Circumpolar ocean stability on Mars 3 Gy ago - Supplementary Material

Frédéric Schmidt[1,2], Michael J. Way[3,4,5], François Costard[1], Sylvain Bouley[1,2,6], Antoine Séjourné[1], Igor Aleinov[3,7]

December 17, 2021

[1]Université Paris-Saclay, CNRS, GEOPS, 91405, ORSAY, FRANCE [2]Institut Universitaire de France (IUF) [3]NASA/Goddard Institute for Space Studies, 2880 Broadway, NY, NY 10025, USA [4]GSFC Sellers Exoplanet Environments Collaboration, Greenbelt, MD, USA, [5]Theoretical Astrophysics, Department of Physics and Astronomy, Uppsala University, Uppsala, SWEDEN [6]IMCCE – Observatoire de Paris, CNRS-UMR 8028, Paris, France [7]Center for Climate Systems Research, Columbia University, New York, NY 10025, USA

Contents

1 Atmosphere and ocean **1**
1.1 Fields 1
1.2 Return flow 6
1.3 Climatic regions 6
1.4 Mass flux 9
1.5 Convergence to equilibrium 9

2 Geology **12**

1 Atmosphere and ocean

1.1 Fields

Fig. 1, 2, 3 and 4 present the simulated fields of rain precipitation, snow/ice fraction, snow fall precipitation and ocean/land surface temperature averaged over 10 Martian years for a H_2 abundance of 10%. The same figures are plotted for a H_2 abundance of 20% in Fig. 5, 6, 7 and 8.

The ocean net heat flux is represented in Fig. 9. It represents the atmosphere warming due to the circulating ocean.

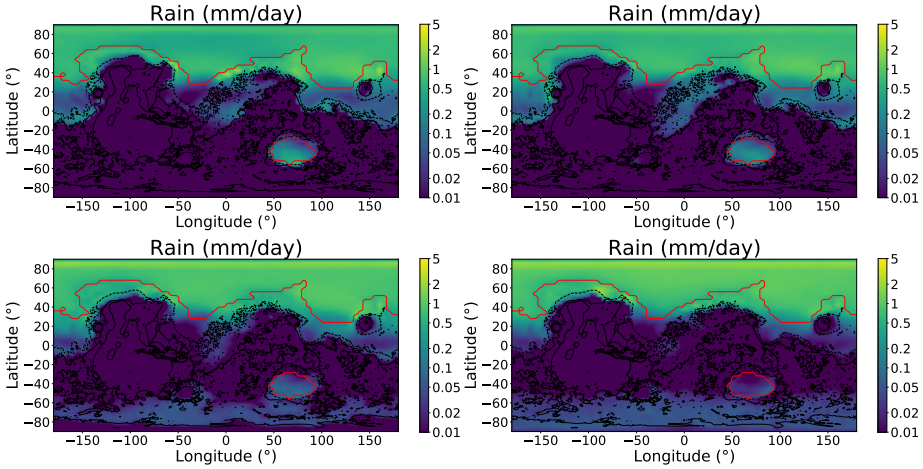


Figure 1: Rain precipitation (in log scale) for H_2=10% for obliquity 0°, 20°, 40° and 60° from top left to bottom right.

Black contour lines are elevation at -2000, 0, 2000 and 8000 meters. The red contour line is the shoreline at -3900 meters.

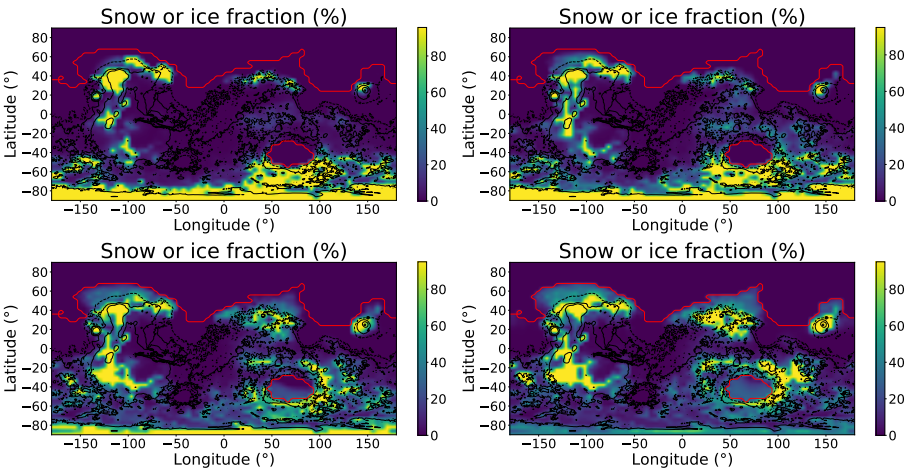


Figure 2: Snow/Ice fraction for H_2=10% for obliquity 0°, 20°, 40° and 60° from top left to bottom right.

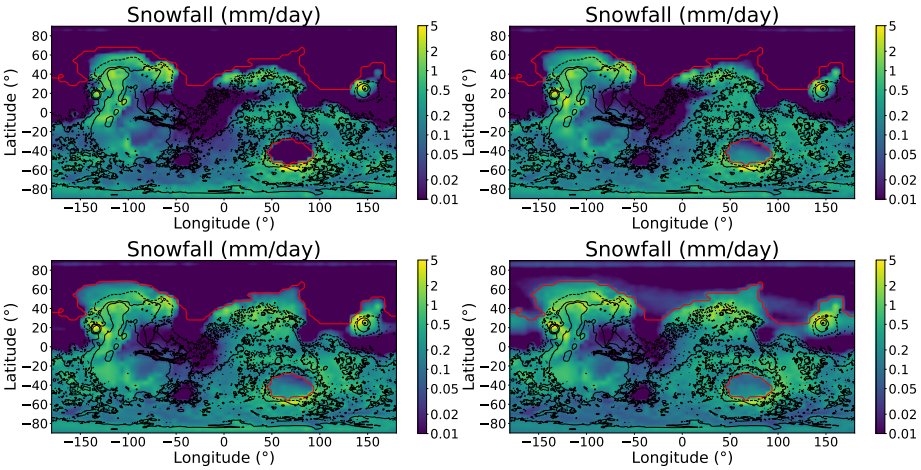


Figure 3: Snow fall precipitation (in log scale) for H_2=10% for obliquity 0°, 20°, 40° and 60° from top left to bottom right.

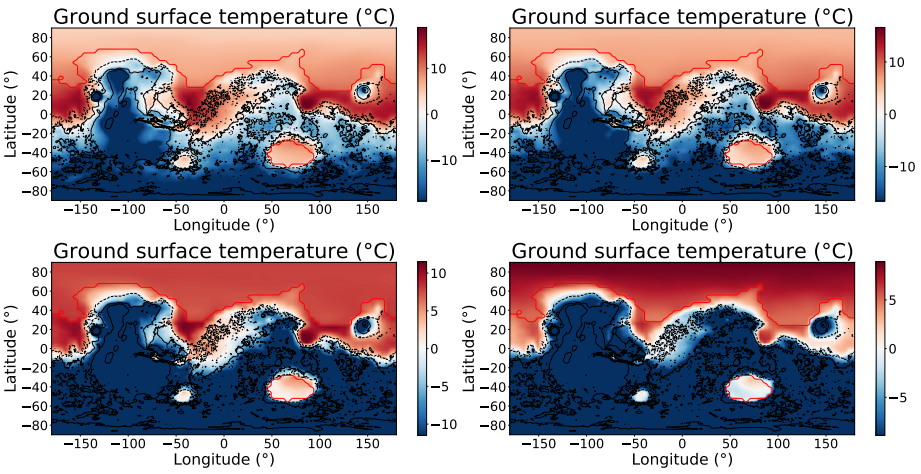


Figure 4: Land/ocean surface temperature for H_2=10% for obliquity 0°, 20°, 40° and 60° from top left to bottom right.

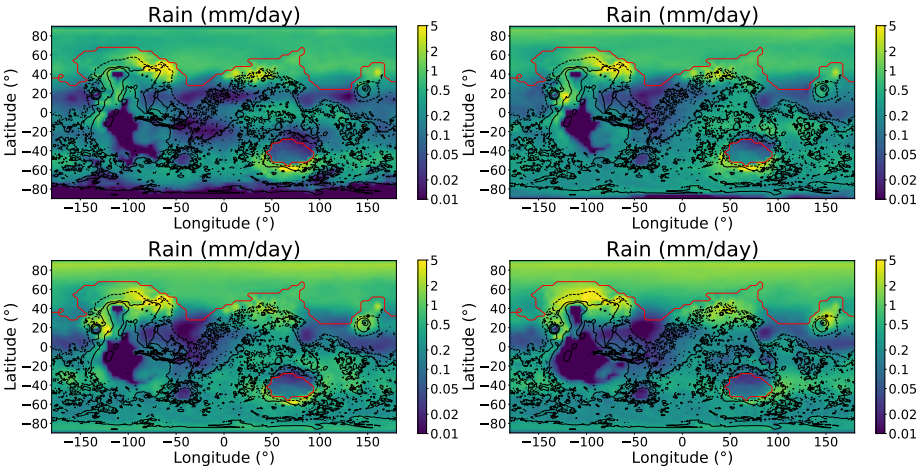


Figure 5: Rain precipitation (in log scale) for H_2=20% for obliquity 0°, 20°, 40° and 60° from top left to bottom right.

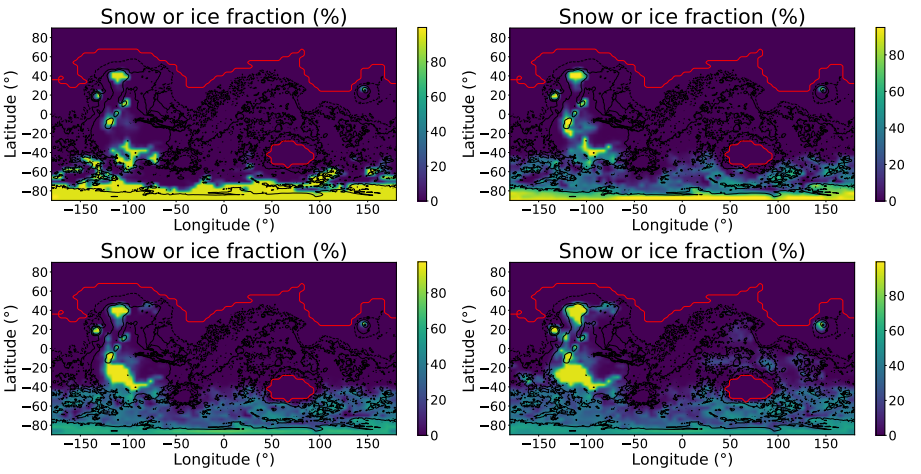


Figure 6: Snow/Ice fraction for H_2=20% for obliquity 0°, 20°, 40° and 60° from top left to bottom right.

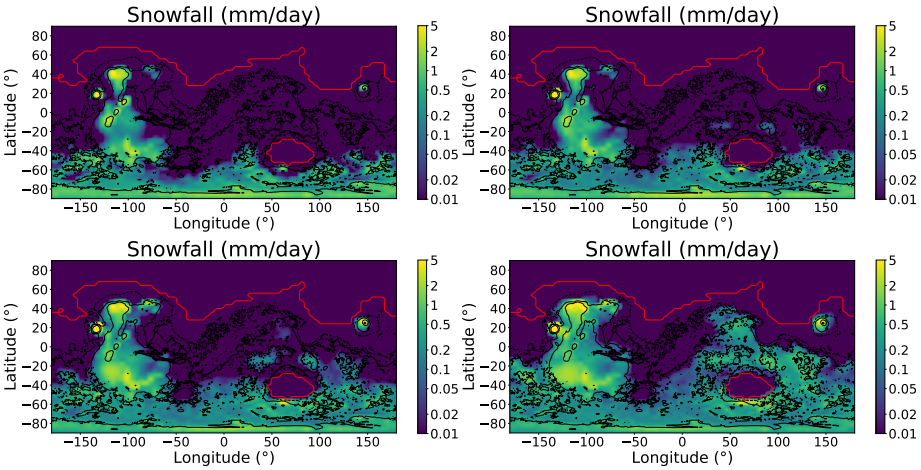


Figure 7: Snow fall precipitation (in log scale) for H_2=20% for obliquity 0°, 20°, 40° and 60° from top left to bottom right.

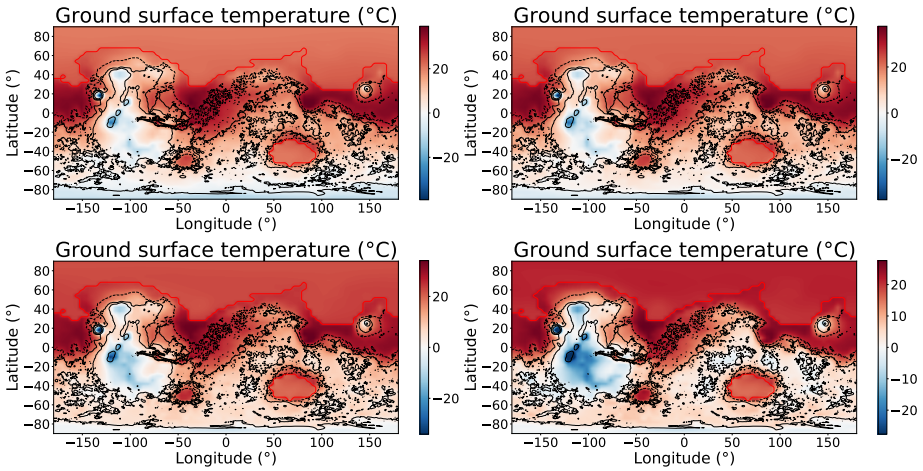


Figure 8: Land/ocean surface temperature for H_2=20% for obliquity 0°, 20°, 40° and 60° from top left to bottom right.

1.2 Return flow

Figure 10 shows the return flow from the icy highlands to the oceans. The simplified mass flux is estimated by restricting snow accumulation to 2 m of H_2O. Any excess is immediately redistributed over the ocean to maintain conservation of water in the system. In all cases, this return flow is very localized to particular regions on Mars (around Hellas, at the top of the volcanoes Alba Patera, Tharsis and Elysium) and not in the full southern hemisphere. The accumulation here is such that a glacier should develop and flow down back to the ocean.

1.3 Climatic regions

Table 1 indicates the mean surface temperature, the mean ocean temperature and the altitude of the 0°C isotherm for two model runs at 1 bar with H_2 content of 10% and 20% and four different obliquities (0°, 20°, 40° and 60°). One can clearly see that H_2 of 10% versus 20% has a major effect. When H_2 is around 10%, as noticed by previous studies [2, 4], the average surface temperature is slightly below 0°C. Nevertheless, thanks to the coupled atmosphere/ocean model, the ocean is stable from freezing with a mean surface ocean temperature > 0°C.

The shoreline is set at -3900 meters corresponding to a surface fraction of 16% of total Mars. Table 2 indicates the surface fraction of each climatic regions (Icy Highlands, Wet Lowland and ocean) as a function of H_2 and obliquity. For H_2=10%, icy highlands dominate but for H_2=20%, wet lowlands dominate.

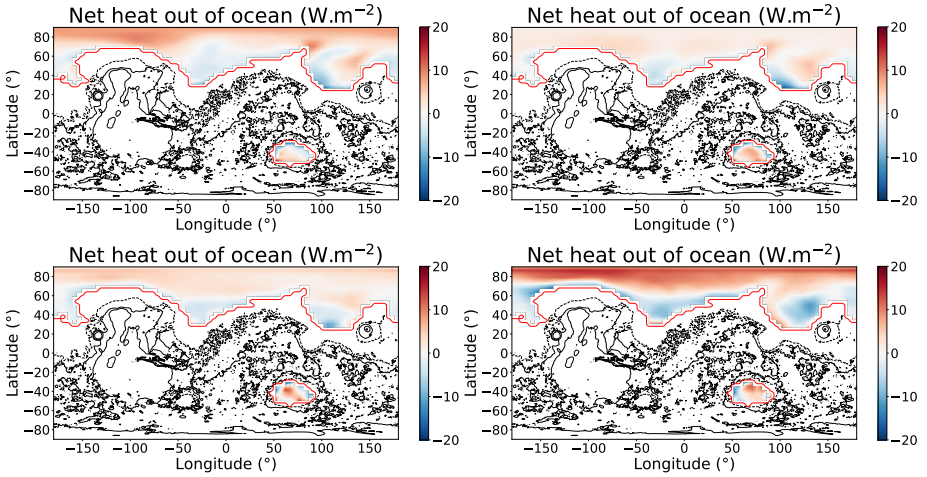


Figure 9: Ocean net heat flux (<0 for heat from the atmosphere to the ocean, >0 for heat toward the atmosphere) for H_2=10% for obliquity 0°, 20°, 40° and 60° from top left to bottom right.

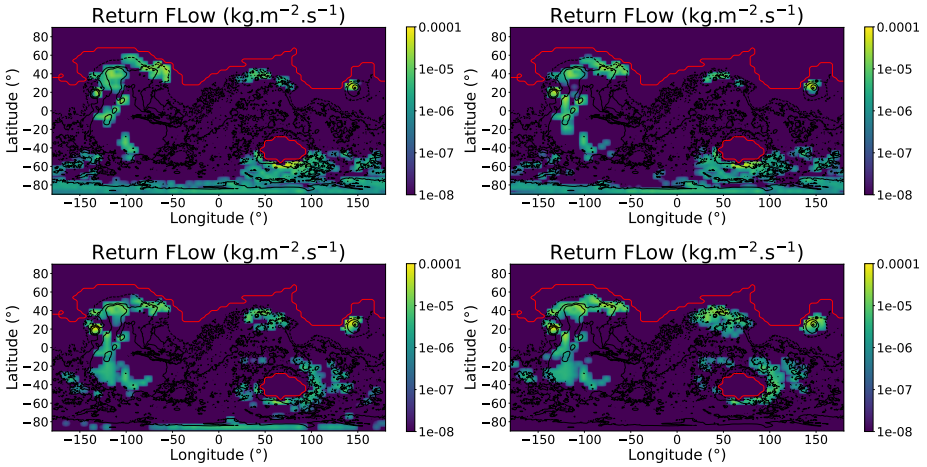


Figure 10: Return flow (in log scale) for H_2=10% and for obliquity 0°, 20°, 40° and 60° from top left to bottom right.

CIRCULATING OCEAN	H_2=10%				H_2=20%			
Obliquity	0°	20°	40°	60°	0°	20°	40°	60°
Simulation	01	02	03	04	05	06	07	08
Average temperature (°C)	-2.9	-4.5	-7.2	-10.3	17.3	16.9	14.8	10.3
Ocean temperature (°C)	7.1	7.0	7.2	6.1	22.0	22.6	22.3	20.4
Land temperature (°C)	-4.8	-6.8	-9.9	-13.4	16.4	15.8	13.4	8.4
Altitude of the 0° isotherm (m)	-680	-1010	-2030	-3060	2060	2260	2660	2230
SLAB OCEAN	H_2=10%				H_2=20%			
Obliquity	0°	20°	40°	60°	0°	20°	40°	60°
Simulation	09	10	11	12	13	14	15	16
Average temperature (°C)	-3.2	-5.7	-8.9	-12.4	16.8	16.2	13.6	8.3
Ocean temperature (°C)	6.8	6.0	5.4	3.7	21.8	22.2	21.0	18.1
Land temperature (°C)	-5.1	-8.0	-11.7	-15.4	15.9	15.1	12.2	6.5
Altitude of the 0° isotherm (m)	-770	-1380	-2750	-3220	1970	2020	2490	1790

Table 1: Mean temperature and altitude of the 0°C isotherm for H_2=10% and 20% and for circulating/slab ocean

CIRC. OCEAN	H_2=10%				H_2=20%			
Obliquity	0°	20°	40°	60°	0°	20°	40°	60°
Simulation	01	02	03	04	05	06	07	08
Icy highland	**52.0**	**55.9**	**62.1**	**71.7**	8.5	6.8	7.3	15.0
Wet lowland	32.3	28.4	22.1	13.5	**76.3**	**78.0**	**77.5**	**69.7**
Ocean	16.2	16.2	16.2	16.2	16.2	16.2	16.2	16.2
SLAB OCEAN	H_2=10%				H_2=20%			
Obliquity	0°	20°	40°	60°	0°	20°	40°	60°
Simulation	09	10	11	12	13	14	15	16
Icy highland	**52.6**	**57.5**	**66.4**	**77.1**	9.8	7.8	8.5	21.3
Wet lowland	31.8	26.8	18.0	8.6	**74.9**	**77.0**	**76.3**	**63.3**
Ocean	16.2	16.2	16.2	16.2	16.2	16.2	16.2	16.2

Table 2: Surface fraction in % of each type of terrain Icy highland, Wet lowland and Ocean for H_2=10% and 20% and for circulating/slab ocean.

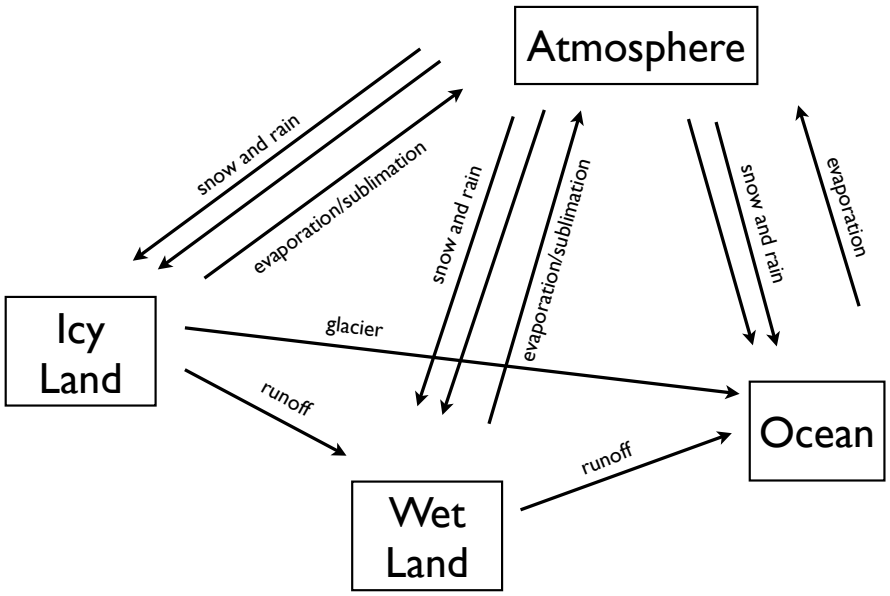


Figure 11: Scheme of the climate system box modeling, with reservoirs and fluxes.

1.4 Mass flux

Figure 11 represents a box model of the climatic system. The fluxes are estimated for each obliquity and H_2 amounts as represented in tables 3 to 10. Errors in the balance are less than 5% of the maximum flux in the box, due to incomplete GCM diagnostics, from salinity changes and numerical rounding.

1.5 Convergence to equilibrium

As an illustration, figure 12 shows the convergence toward radiative equilibrium of two GCM runs from two global model diagnostics: average temperature and

	0°	20°	40°	60°
Evaporation	-6.80e+15	-8.77e+15	-1.06e+16	-1.19e+16
Rain	9.08e+13	1.59e+14	5.39e+14	9.52e+14
Snow	9.44e+15	1.12e+16	1.34e+16	1.47e+16
Runoff to Wet lowland	-1.48e+13	-2.72e+14	-6.54e+14	-8.34e+14
Glacier to Ocean	-2.72e+15	-2.31e+15	-2.67e+15	-2.97e+15
Balance	5.00e-01	-5.00e-01	1.00e+00	0.90e+00

Table 3: Icy highland fluxes for H_2=10% in kg/Earth year

	0°	20°	40°	60°
Evaporation	-3.73e+15	-3.45e+15	-3.02e+15	-2.33e+15
Rain	3.06e+15	2.83e+15	2.44e+15	1.87e+15
Snow	1.00e+15	1.02e+15	1.15e+15	8.47e+14
Runoff from Icy highland	1.48e+13	2.72e+14	6.54e+14	8.34e+14
Runoff to Ocean	-3.46e+14	-6.79e+14	-1.22e+15	-1.22e+15
Balance	-1.31e+12	-9.98e+11	-1.71e+12	-2.67e+12

Table 4: Wet lowland fluxes for H_2=10% in kg/Earth year

	0°	20°	40°	60°
Evaporation	-7.67e+15	-8.13e+15	-9.78e+15	-1.12e+16
Rain	4.58e+15	5.03e+15	5.72e+15	6.33e+15
Snow	2.08e+12	9.12e+13	1.26e+14	2.35e+14
Glacier	2.72e+15	2.31e+15	2.67e+15	2.97e+15
Runoff	3.46e+14	6.82e+14	1.23e+15	1.36e+15
Sea ice	0.00e+00	0.00e+00	-3.28e+10	-6.29e+10
Balance	-2.56e+13	-2.09e+13	-4.31e+13	-3.37e+14

Table 5: Ocean fluxes for H_2=10% in kg/Earth year

	0°	20°	40°	60°
Evaporation from Icy highland	6.80e+15	8.77e+15	1.06e+16	1.19e+16
Rain to Icy highland	-9.08e+13	-1.59e+14	-5.39e+14	-9.52e+14
Snow to Icy highand	-9.44e+15	-1.12e+16	-1.34e+16	-1.47e+16
Evaporation from Wet lowland	3.73e+15	3.45e+15	3.02e+15	2.33e+15
Rain to Wet lowland	-3.06e+15	-2.83e+15	-2.44e+15	-1.87e+15
Snow to Wet lowland	-1.00e+15	-1.02e+15	-1.15e+15	-8.47e+14
Evaporation from Ocean	7.67e+15	8.13e+15	9.78e+15	1.12e+16
Rain to Ocean	-4.58e+15	-5.03e+15	-5.72e+15	-6.33e+15
Snow to Ocean	-2.08e+12	-9.12e+13	-1.26e+14	-2.35e+14
Balance	2.70e+13	2.47e+13	5.73e+13	4.77e+14

Table 6: Atmosphere fluxes for H_2=10% in kg/Earth year

	0°	20°	40°	60°
Evaporation	-2.20e+15	-2.21e+15	-2.66e+15	-4.99e+15
Rain	2.83e+14	5.64e+14	7.49e+14	1.45e+15
Snow	4.22e+15	3.95e+15	4.77e+15	7.71e+15
Runoff to Wet lowland	-1.08e+14	-5.79e+14	-5.37e+14	-1.29e+15
Glacier to Ocean	-2.20e+15	-1.73e+15	-2.33e+15	-2.87e+15
Balance	-2.50e-01	0.00e+00	0.00e+00	0.00e+00

Table 7: Icy highland fluxes for H_2=20% in kg/Earth year

	0°	20°	40°	60°
Evaporation	-1.23e+16	-1.48e+16	-1.57e+16	-1.51e+16
Rain	1.41e+16	1.64e+16	1.75e+16	1.62e+16
Snow	1.45e+15	2.42e+15	3.84e+15	4.93e+15
Runoff from Icy highland	1.08e+14	5.79e+14	5.37e+14	1.29e+15
Runoff to Ocean	-3.33e+15	-4.09e+15	-5.72e+15	-7.03e+15
Balance	5.94e+13	5.01e+14	4.32e+14	2.52e+14

Table 8: Wet lowland fluxes for H_2=20% in kg/Earth year

	0°	20°	40°	60°
Evaporation	-9.94e+15	-1.09e+16	-1.41e+16	-1.63e+16
Rain	4.33e+15	4.60e+15	5.55e+15	6.07e+15
Snow	0.00e+00	0.00e+00	0.00e+00	0.00e+00
Glacier	2.20e+15	1.73e+15	2.33e+15	2.87e+15
Runoff	3.33e+15	4.09e+15	5.73e+15	7.04e+15
Sea ice	0.00e+00	0.00e+00	0.00e+00	0.00e+00
Balance	-8.11e+13	-5.18e+14	-4.61e+14	-2.82e+14

Table 9: Ocean fluxes for H_2=20% in kg/Earth year

	0°	20°	40°	60°
Evaporation from Icy highland	2.20e+15	2.21e+15	2.66e+15	4.99e+15
Rain to Icy highland	-2.83e+14	-5.64e+14	-7.49e+14	-1.45e+15
Snow to Icy highand	-4.22e+15	-3.95e+15	-4.77e+15	-7.71e+15
Evaporation from Wet lowland	1.23e+16	1.48e+16	1.57e+16	1.51e+16
Rain to Wet lowland	-1.41e+16	-1.64e+16	-1.75e+16	-1.62e+16
Snow to Wet lowland	-1.45e+15	-2.42e+15	-3.84e+15	-4.93e+15
Evaporation from Ocean	9.94e+15	1.09e+16	1.41e+16	1.63e+16
Rain to Ocean	-4.33e+15	-4.60e+15	-5.55e+15	-6.07e+15
Snow to Ocean	0.00e+00	0.00e+00	0.00e+00	0.00e+00
Balance	2.27e+13	2.23e+13	3.37e+13	4.24e+13

Table 10: Atmosphere fluxes for H_2=20% in kg/Earth year

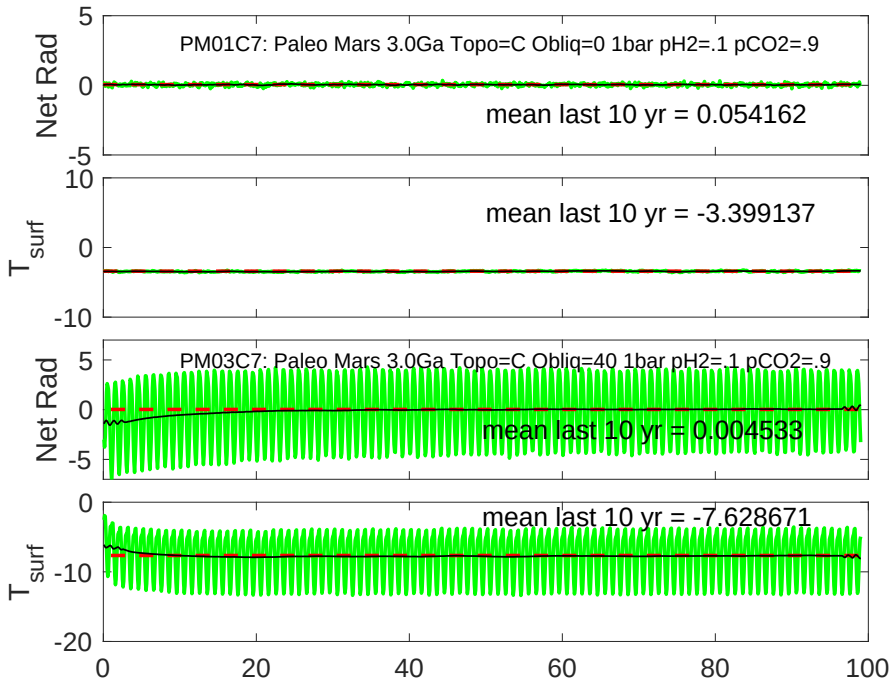


Figure 12: Convergence diagnostics for the last 100 years for (top) Obliquity 0°, H_2=10% (bottom) Obliquity 40°, H_2=10%. Each case represent the mean net radiation (W.m^{-2}) and the average surface temperature (°C). Green line is the monthly average data. The red dashed line is the value of the last 10 years for that diagnostic to allow the reader to see that the GCM is reaching an asymptote (no change as we move forward in time). Black line is a 60 month smoothing of the green line.

net radiation balance. All data used in the article are an average of the last 10 years after equilibrium is reached ($< \pm 0.2$ W.m^{-2} in 10 year net radiation balance). Please note that the bottom two panels in Fig. 12 are a "warm restart" from a similar simulation such that the time to reach equilibrium is quite fast (<100 years).

2 Geology

More recent geological units may cover the 3 Gy old terrain affected by the proposed climate. Figure 13 shows a map of the proposed hydrological cycle scenario with the more recent Amazonian terrains. For example, the pre-Amazonian glacier's head of Kasei Valles [1] is covered by Amazonian geological units. Other glaciers may have also been present but their marks could have

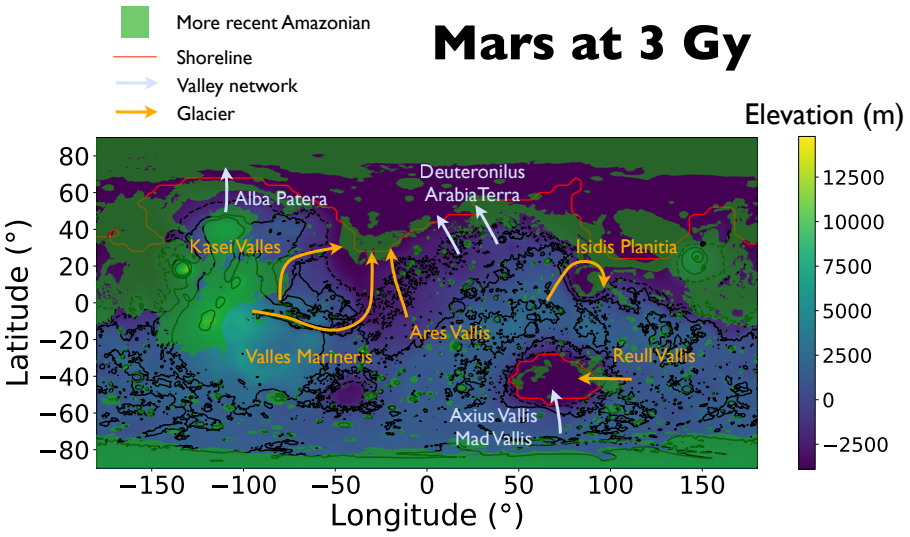


Figure 13: Map of the proposed hydrological cycle scenario in the cold and wet climate in the Hesperian age (3 Ga). The topography is modern without the North Polar Layered Deposits. Geological evidence of past glaciers with return flow to the oceans are highlighted in addition to the limited evidence for high drainage density valley networks. The green background represents the more recent Amazonian terrain covering the area (adapted from [3]).

been hidden by covering materials.

References

[1] John Arfstrom. Equatorial ice sheets of mars, 2020. doi:10.13140/RG.2.2.30127.36004.

[2] A. Kamada, T. Kuroda, Y. Kasaba, N. Terada, H. Nakagawa, and K. Toriumi. A coupled atmosphere–hydrosphere global climate model of early mars: A 'cool and wet' scenario for the formation of water channels. *Icarus*, 338:113567, mar 2020. doi:10.1016/j.icarus.2019.113567.

[3] K. L. Tanaka, Jr. Skinner, J. A., J. M. Dohm, III Irwin, R. P., E. J. Kolb, C. M. Fortezzo, T. Platz, G. G. Michael, and T. M. Hare. Geologic map of Mars. *U.S. Geological Survey Report*, page 3292, July 2014. doi:10.3133/sim3292.

[4] M. Turbet and F. Forget. The paradoxes of the late hesperian mars ocean. *Scientific Reports*, 9(1), apr 2019. doi:10.1038/s41598-019-42030-2.